

Unitarity triangle angles explained: a predictive new quark mass matrix texture

P.F. Harrison^a W.G. Scott^b

^a*Department of Physics, University of Warwick,
Coventry CV4 7AL, United Kingdom.*

^b*Rutherford Appleton Laboratory,
Chilton, Didcot OX11 0QX, United Kingdom.*

E-mail: p.f.harrison@warwick.ac.uk, william.scott@stfc.ac.uk

ABSTRACT: We propose a novel quark mass matrix texture-pair with five free parameters, which fits the four quark mass ratios m_s/m_b , m_d/m_b , m_c/m_t , m_u/m_t , and the four CKM quark mixing observables. The matrices each have one texture zero, but the main innovation here is a “geometric” ansatz exploiting a pair of small complex expansion parameters, based on the geometry of the Unitarity Triangle. The fit to the observables is in good agreement with current experimental values renormalised to $\sim 10^4$ TeV, and offers decisive tests against future high-precision measurements of the unitarity triangle angles at the weak scale. We identify two novel symmetries of these mass matrices which explain the phenomenologically-successful relations $\alpha \equiv \phi_2 \simeq \frac{\pi}{2}$ and $\beta \equiv \phi_1 \simeq \frac{\pi}{8}$.

KEYWORDS: CKM Matrix, Flavour Symmetries, *CP* Violation

ARXIV EPRINT: [2501.18508](https://arxiv.org/abs/2501.18508)

Contents

1	Introduction	1
2	The texture	2
3	Leading-order solution	3
4	Numerical fit to the data	5
5	Constraints	7
6	Symmetries of the mass matrices	7
7	Discussion	10
A	Analytic NLO solutions	11

1 Introduction

There has been a long history of textures proposed for the quark mass/Yukawa matrices (MMs), both as stand-alone ansatze, and/or as the result of (or motivation for) models which can constrain them. The traditional guiding principle for such textures has been to reduce the number of free parameters (a priori 36) to a number smaller than the ten observables, in order to find predictive constraints among the measurable quantities, especially relationships between the quark masses and mixings [1][2][3][4], which each manifest marked hierarchical structure. Methods have included using symmetries to enforce texture-zeroes [5], and/or mechanisms to produce a hierarchy among the matrix elements [6]. Recently, ideas have turned to the realm of modular forms [7][8], where again approaches have been found to enforce zeroes [9] and/or hierarchies [10]. We introduce here a new MM texture based purely on the CKM and quark mass phenomenology, which is modestly predictive, fits the data, and has some novel and potentially interesting features.

The closeness of the (beauty-down) Unitarity Triangle (UT) [11][12] to a right-angled triangle is striking [13][14][15], and it is also notable that its three internal angles [16],¹

$$\alpha \equiv \phi_2 = (91.6 \pm 1.4)^\circ; \quad \beta \equiv \phi_1 = (22.6 \pm 0.4)^\circ; \quad \gamma \equiv \phi_3 = (65.7 \pm 1.3)^\circ, \quad (1.1)$$

are very close to the aesthetically appealing triplet [17]:

$$(\alpha, \beta, \gamma) \simeq (\alpha_0, \beta_0, \gamma_0) \equiv \left(\frac{\pi}{2}, \frac{\pi}{8}, \frac{3\pi}{8}\right). \quad (1.2)$$

¹We use the measured value for β and the CKM fit values [16] for α and γ , since these give the smallest uncertainties.

We consider the possibility that these suggestive angles may be significant, not merely as numerical coincidences, but taken together, as a clue to what may lie behind the quark flavour structure. So, we set-out from the start to build them into a MM texture and we later show that they can be enforced by a pair of symmetries among the MMs. This approach is successful, at least in terms of reducing the number of free parameters needed to describe the data, as we will see. We first emphasise that our ansatz does not assure exact equality in eq. (1.2), but rather, we adopt analogous equalities into the (arguably more fundamental) MMs, which yield, after diagonalisation, the approximate equalities seen at the level of the UT in the equation.

2 The texture

The proposed new texture is common to both the up and down quark MMs, constraining them relative to those of the SM. Without loss of generality, we take the MMs to be Hermitian. We adopt the popular texture zero in the 13 and 31 elements [1][2][3][4], so that the smallest mixing elements result from the non-commutation of the (small) diagonalising transformations in the 12 and 23 subspaces. In order both to introduce viable hierarchies among the MMs' elements, and to include CP violation, we adopt two small, complex expansion parameters,² λ_u and λ_d , powers of which are inserted into the up and down quark MMs respectively, each playing a role similar to Wolfenstein's λ parameter in the CKM matrix [18], but distinct for each of the two MMs. Thus, we express both MMs as follows:

$$M_q = n_q M_q^0 \equiv n_q \begin{pmatrix} c_q \lambda_q^4 & b \lambda_q^3 & 0 \\ \sim & b \lambda_q^2 & A_0 \lambda_q^2 \\ 0 & \sim & 1 \end{pmatrix}, \quad q = u, d, \quad (2.1)$$

with the normalisations $n_q \simeq m_t, m_b$ for $q = u, d$ respectively, the real coefficients (A_0, b, c_u, c_d) are of magnitude $\lesssim \mathcal{O}(1)$, and the ' \sim ' symbol means "the complex conjugate of the diagonally-opposite entry". The equality in the coefficients between the 12 and 22 elements is conventional, any a priori difference having been absorbed into the normalisations of λ_q , by virtue of the different powers involved.

The overall normalisations of the λ_q ($q = u, d$) are free to vary, but we anticipate that their complex sum has magnitude close to the value of Wolfenstein's expansion parameter:

$$|\lambda_d + \lambda_u| \equiv \lambda_0 = \lambda + \mathcal{O}(\lambda^3). \quad (2.2)$$

The absolute phases of the λ_q are unobservable, specific choices corresponding to particular phase conventions related by simultaneous, common rephasings of both (see below). An inequality among the λ_q magnitudes, $\lambda_u < \lambda_d$, is anticipated to ensure that the up-like mass hierarchy is more extreme than the down-like one, and in order to reproduce the

²Throughout this paper, where ambiguity can arise, bold font is used to denote complex quantities, and the corresponding light font symbols, their moduli. Complex conjugation is indicated by the conventional * symbol.

triplet of experimental results for the UT angles, eq. (1.2), we take the ratio of the λ_q to be the exact complex *constant*:

$$\frac{\lambda_u}{\lambda_d} = -i \tan \frac{\pi}{8}. \quad (2.3)$$

The constraint, eq. (2.3), is the most significant innovation in this paper. Specifically, in our texture, $(\lambda_u/\lambda_d)^*$ is identifiable in leading approximation with the complex ratio of the two sloped sides of the UT as we show below. Thus $\arg(\lambda_u/\lambda_d)$ corresponds to the supplement of the UT angle α , the constrained value ensuring $\alpha \simeq \frac{\pi}{2}$; the ratio $|\lambda_u/\lambda_d|$ then corresponds similarly to $\tan\beta$ (while simultaneously determining the asymmetry between the mass hierarchies in the two charge sectors). Thus eq. (2.3) applied in our texture, eq. (2.1), yields eq. (1.2). Moreover, the precise values for the ratio asserted by eq. (2.3) imply and are implied by two novel symmetries of the M_q^0 , as we will also show.

The MM texture, eq. (2.1), uses five free parameters, A_0, b, c_u, c_d and λ_0 to fit the three quark mixing angles, the CP phase, and the four quark mass ratios, making it modestly predictive. A more general parameterisation would allow the (A_0, b) parameters to be different for $q = u, d$, but we find that *it is possible to fit all the quark mass and mixing observables with the parameter-pair (A_0, b) , common to both mass matrices*. Thus an *up/down* (weak isospin) reflection symmetry is respected by the real parameters (A_0, b) , and broken only by the λ_q , the pair of parameters c_q which govern m_u and m_d , and by the matrix normalisations, n_q in eq. (2.1).

3 Leading-order solution

As usual we diagonalise the M_q by the unitary transformations:

$$U^q M_q U^{q\dagger} = \text{diag}(m_1^q, m_2^q, m_3^q), \quad q = u, d, \quad (3.1)$$

but since the diagonalisation is insensitive to the normalisation of M_q , we work with the dimensionless M_q^0 , eq. (2.1). The off-diagonal elements are small compared with the corresponding diagonal ones, so we can use small-angle approximations. We find at leading order in λ_0 that the largest eigenvalue of the M_q^0 is unity, while the second eigenvalue is given by:

$$\frac{m_2^q}{m_3^q} = b\lambda_q^2, \quad q = u, d, \quad (3.2)$$

also at leading order in λ_0 . Consecutive 2×2 diagonalisations can be made in the 23 and 12 sub-spaces leading to the U^q each being composed of a product of two 2D (generally complex) rotation matrices. Since rotations about different axes do not commute, small entries are induced in the 13 elements of U^q . At leading order:

$$U^q \simeq \begin{pmatrix} 1 & \pm\lambda_q & A_0\lambda_q^3 \\ \mp\lambda_q^* & 1 & -A_0\lambda_q^2 \\ 0 & A_0\lambda_q^{2*} & 1 \end{pmatrix}, \quad q = u, d, \quad (3.3)$$

where the upper sign³ is for the $q = u$ case and the lower for $q = d$. Combining both diagonalising matrices, we obtain the CKM matrix at leading order in λ_0 (note eq. (2.2)):

$$V_{CKM} = U^u U^{d\dagger} \simeq \begin{pmatrix} 1 & \lambda_d + \lambda_u & A_0 \lambda_u \delta \lambda^2 \\ -(\lambda_d + \lambda_u)^* & 1 & A_0 \delta \lambda^2 \\ A_0 \lambda_d^* \delta \lambda^{2*} & -A_0 \delta \lambda^{2*} & 1 \end{pmatrix} \sim \begin{pmatrix} 1 & \lambda_0 & A_0 \lambda_0^2 \lambda_u \\ -\lambda_0 & 1 & A_0 \lambda_0^2 \\ A_0 \lambda_0^2 \lambda_d^* & -A_0 \lambda_0^2 & 1 \end{pmatrix}, \quad (3.4)$$

where⁴

$$\delta \lambda^2 \equiv \lambda_d^2 - \lambda_u^2 \Rightarrow |\delta \lambda^2| = \lambda_0^2. \quad (3.5)$$

The first matrix in Eq. (3.4) is independent of the choice of phase convention, while the second applies in the PDG phase convention where V_{us} and V_{cb} are real. We can now compare the off-diagonal elements with their Wolfenstein equivalents, to obtain in this convention:

$$\lambda_u \simeq \lambda(\rho - i\eta) = V_{ub}/A\lambda^2 \quad (3.6)$$

$$\lambda_d \simeq \lambda(1 - \rho + i\eta) = V_{td}^*/A\lambda^2 \quad (3.7)$$

$$A_0 \simeq A, \quad (3.8)$$

where λ , ρ , η and A are the Wolfenstein parameters [18] (and eq. (3.8) explains our choice of symbol A_0 in eq. (2.1)). This confirms that at leading order, λ_u^* and λ_d^* are each proportional to one of the ‘‘sloped’’ sides of the UT (since, in the CKM phase convention, $V_{ud} \simeq V_{tb} \simeq 1$). We can thus immediately justify the claims made below eq. (2.2):

$$\frac{\lambda_u}{\lambda_d} = \frac{V_{ub}}{V_{td}^*}, \quad \text{cf. } \alpha \equiv \arg\left(-\frac{V_{td}V_{tb}^*}{V_{ud}V_{ub}^*}\right), \quad (3.9)$$

$$\Rightarrow \arg\left(\frac{\lambda_u}{\lambda_d}\right) = \arg\left(\frac{V_{td}}{V_{ub}^*}\right) \simeq \pi - \alpha \quad \text{and} \quad \left|\frac{\lambda_u}{\lambda_d}\right| \simeq \tan\beta, \quad (3.10)$$

where the last near-equality is a consequence of the near right-angle in the resulting UT (the definition of α is from the PDG [16]).

Still in the PDG phase convention where $\lambda_d + \lambda_u = \lambda_0$, it is useful to define the complex constants:⁵

$$\mathbf{z}_0 \equiv \lambda_u^*/\lambda_0 = i s_0 e^{-i\beta_0} = \rho_0 + i\eta_0, \quad (3.11)$$

$$\bar{\mathbf{z}}_0 \equiv \lambda_d^*/\lambda_0 = c_0 e^{-i\beta_0} = 1 - \mathbf{z}_0, \quad (3.12)$$

where $\beta_0 \equiv \frac{\pi}{8}$ was defined in eq. (1.2), and:⁶

$$s_0 \equiv \sin\beta_0; \quad c_0 \equiv \cos\beta_0; \quad \eta_0 = s_0 c_0 = \frac{1}{2\sqrt{2}} \quad \text{and} \quad \rho_0 = s_0^2. \quad (3.13)$$

³Eq. (3.3) applies exactly as shown, only in the phase convention in which λ_d is real and λ_u is imaginary, the extra factor -1 in the $q = u$ case arising as the phase of two cancelled powers of λ_u .

⁴ $|\lambda_d - \lambda_u| = |\lambda_d + \lambda_u|$ due to the λ_u/λ_d phase difference of $\frac{\pi}{2}$.

⁵The ‘‘bar’’ in $\bar{\mathbf{z}}_0$ is simply to identify this variable as the one-complement of \mathbf{z}_0 and should not be confused with the bar appearing above the ‘‘reduced’’ Wolfenstein parameters $\bar{\rho}$ and $\bar{\eta}$.

⁶ $s_0 = \frac{1}{2}\sqrt{2 - \sqrt{2}} = 0.383$ and $c_0 = \frac{1}{2}\sqrt{2 + \sqrt{2}} = 0.924$.

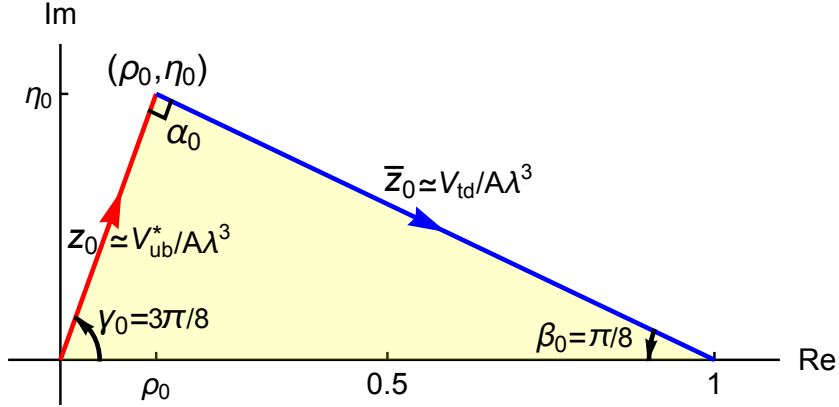


Figure 1. Leading-order Unitarity Triangle used as input to textures. The UT extracted after diagonalisation of the mass matrices is congruent to it at leading order in small quantities. The angles $(\alpha_0, \beta_0, \gamma_0)$ are defined in eq. (1.2), and $(\rho_0, \eta_0) = (0.146, 0.354)$.

We illustrate eqs. (3.6)-(3.10) in figure 1, which shows the leading-order UT (“LO-UT”) whose angles and sides are used as input to our texture, eq. (2.1), which ensures that an approximately congruent UT results after diagonalisation. The apex of the standard UT is simply given by [16][19]:

$$\bar{\rho} + i\bar{\eta} \simeq \mathbf{z}_0. \quad (3.14)$$

Our working so far has been in the small-angle limit, i.e. ignoring cosines of the quark mixing angles, so that we cannot assume a relative accuracy better than $1 - \cos(\theta_C) \sim \lambda^2/2 \sim 2.5\%$. Thus, we have not yet needed to distinguish between the two pairs of similar parameters, (ρ, η) [18] and $(\bar{\rho}, \bar{\eta})$ [19], which differ by just this fraction [16]. For the numerical results below, following the PDG [16], we choose to work with $(\bar{\rho}, \bar{\eta})$. The full next-to leading order (NLO) algebraic solutions of the texture for the mixings and mass ratios are given in the Appendix.

4 Numerical fit to the data

For the fit to the data, a full diagonalisation is performed at high numerical precision. The CKM parameters are taken from the latest PDG compilation [16]. Significant recent progress in quark mass determinations using lattice QCD [20] has led to dramatic reductions in the uncertainties on the quark mass ratios (which we take as experimental inputs⁷). We follow the approach of [21], updating the inputs with the latest lattice determinations compiled in the PDG review on quark masses [16]. These inputs are initially quoted in the second column of table 1 renormalised to the scale $\mu = m_t = 173.1$ GeV in the $\overline{\text{MS}}$ scheme. A χ^2 fit to the data is performed, varying the five free parameters of the MMs to find their preferred values, which are given in the table caption.

⁷Lattice quark mass determinations are calibrated to experimentally-determined meson masses.

Observable	Experimental	Input Renorma-	Fitted Value	Pull
	Input at m_t	lised to 10^4 TeV	at 10^4 TeV	
$ m_u/m_c (\times 10^3)$	2.00 ± 0.05	Unchanged	2.00	0.00
$ m_d/m_s (\times 10^2)$	4.97 ± 0.06	"	4.97	0.03
$m_c/m_t(\times 10^3)$	3.67 ± 0.04	3.46 ± 0.03	3.46	-0.01
$m_s/m_b(\times 10^2)$	1.854 ± 0.007	1.968 ± 0.008	1.968	0.02
λ	0.22501 ± 0.00068	Unchanged	0.22499	-0.03
A	$0.826^{+0.016}_{-0.015}$	$0.877^{+0.017}_{-0.016}$	0.876	-0.09
$\bar{\rho}$	0.1591 ± 0.0094	Unchanged	0.1519	-0.76
$\bar{\eta}$	$0.3523^{+0.0073}_{-0.0071}$	"	0.3477	-0.65
Total χ^2/dof	—	—	1.01/2	—
$\alpha(^{\circ})$	91.6 ± 1.4	Unchanged	91.3	-0.21
$\beta(^{\circ})$	22.6 ± 0.4	"	22.3	-0.75
$\gamma(^{\circ})$	65.7 ± 1.3	"	66.4	0.54
$J_{CP}(\times 10^5)$	$3.12^{+0.13}_{-0.12}$	$3.49^{+0.15}_{-0.13}$	3.45	-0.29

Table 1. Comparison of observed quark mass ratios and mixing observables at m_t and renormalised to 10^4 TeV, with those obtained by the fit to the textures, eq. (2.1). J_{CP} is Jarlskog’s CP -violating invariant. The values of the fitted parameters are: $A_0 = 0.854$, $b = 0.462$, $c_d = -0.040$, $c_u = 0.344$ and $\lambda_0 = 0.22646$.

The fit to the data renormalised at the weak scale ($\mu = m_t$, not shown), is excluded by its χ^2/dof ($\simeq 100/3$). However, the lack of observations of new physics at around this scale makes it unlikely anyway that a MM texture applies at this scale. Several of the fitted observables evolve with renormalisation scale, and the rate and direction of this evolution in the SM are well-known [22][23][24][25][26]. It is thus possible that our texture might more naturally apply at some higher energy scale, so we have scanned the SM evolution of the relevant observables up to the GUT scale, to investigate this possibility. The best fit is at a scale $\mu \sim 10^4$ TeV with a $\chi^2/dof^8 \simeq 1.0/2$ and a ± 1 standard deviation width of \sim a factor 3 on either side, giving the range $\mu \sim (0.3 \rightarrow 3) \times 10^4$ TeV.

The full fit results for the preferred solution are shown in table 1 where the second column shows the input data, the third gives the same inputs renormalised to the best fit scale, $\mu \sim 10^4$ TeV, the fourth gives the fitted values of the observables, while the fifth gives the individual pulls compared with the input observables at the best fit scale. The χ^2 is calculated summing over those parameters above the dashed line for all observables renormalised to the best fit scale. Observables shown below the total χ^2 line are not independent, and are not used in the fit, but are given for completeness, since the fitted

⁸While the scale μ is not a parameter of the texture, we include it in this count of fit parameters.

values may be tested more precisely than at present by future measurements.

As is usual, the signs of the masses are unphysical, so that different signs of the fitted quark mass ratios must be allowed for in the fit. Only two of the possible sign permutations have viable χ^2 values, namely those with either sign of m_u/m_c , with m_d/m_s negative and the other mass ratios positive. These two solutions are mutually unresolved, being almost degenerate in χ^2 , and in the values of all fit parameters except c_u , which controls m_u/m_c . Thus to avoid repetition, we have reported only the fit for the smaller value of c_u (with m_u/m_c negative). The fits for other permutations of mass-signs are significantly disfavoured by their χ^2 values.

5 Constraints

Naturally, with five parameters and eight observables, there are, in principle, three constraints among the observables. At LO in λ_0 , they are independent of any of the parameters, whereas at higher orders, they become parameter-dependent. From eq. (3.2) and eqs. (3.11)-(3.14) we combine to give the LO constraints:

$$\frac{m_c m_b}{m_t m_s} = \frac{\lambda_u^2}{\lambda_d^2} = \tan^2 \frac{\pi}{8} = 0.172, \text{ c.f. } 0.177 \pm 0.002(\text{exp}) = 0.176(\text{fit}); \quad (5.1)$$

$$\bar{\eta} = \eta_0 \equiv \frac{1}{2\sqrt{2}} = 0.354, \text{ c.f. } 0.352 \pm 0.007(\text{exp}) = 0.348(\text{fit}); \quad (5.2)$$

$$\bar{\rho} + \bar{\eta} = \rho_0 + \eta_0 \equiv \frac{1}{2}, \text{ c.f. } 0.511 \pm 0.012(\text{exp}) = 0.500(\text{fit}), \quad (5.3)$$

where eq. (5.1) is a scale-dependent prediction and eqs. (5.2)-(5.3) are scale-independent. The numerical results, given for comparison above, are from table 1 and are given at the best fit scale, $\mu \sim 10^4$ TeV. The analytic NLO formulae are given in the Appendix, eqs. (A.3)-(A.6), and can be combined to provide a better match to the fitted values quoted above. Finally, we note the suggestive similarity between eq. (5.1) and the phenomenologically successful prediction for the neutrino mass ratio: $\frac{m_2}{m_3} = \tan^2 \frac{\pi}{8}$ in [27].

6 Symmetries of the mass matrices

The texture, eqs. (2.1)-(2.3), and its fit, table 1, are the main results of this paper. Having established that a viable fit to the data is possible for this texture, we identify the two invariance properties of the MMs which realise the complex constant, λ_u/λ_d , defined in eq. (2.3).

The ratio λ_u/λ_d involves a parameter from each MM, so that a regularity therein cannot be reflected in either matrix alone. The UT is significant in providing a diagrammatic representation of a relationship *between* the MMs and we will find it particularly useful in illustrating the symmetries inherent in our MM-pair. We first recall that a *CP* transformation is effected by a simple complex conjugation: here, simply $\mathbf{z}_0 \rightarrow \mathbf{z}_0^*$, $\bar{\mathbf{z}}_0 \rightarrow \bar{\mathbf{z}}_0^*$. The Jarlskog invariant, J_{CP} , flips sign, the UT is reflected in the real axis, and other observables are preserved. Naturally, a very poor fit to the data results, due to the resulting wrong sign of $\bar{\eta}$. Less obviously, with our textures, under either $\mathbf{z}_0 \rightarrow -\mathbf{z}_0$ or $\bar{\mathbf{z}}_0 \rightarrow -\bar{\mathbf{z}}_0$

(but not both), we also obtain a sign-flip of J_{CP} with no other consequences. Thus the simultaneous application of both $z_0 \rightarrow -z_0$ and a CP transformation cancel each other out, making the combined transformation a symmetry of our MM-pair. Analogously, simultaneous application of $\bar{z}_0 \rightarrow -\bar{z}_0$ and CP also leave the observables invariant and are another manifestation of their symmetry.

The situation is illustrated in figure 2, where the LO-UT is again shaded yellow, its

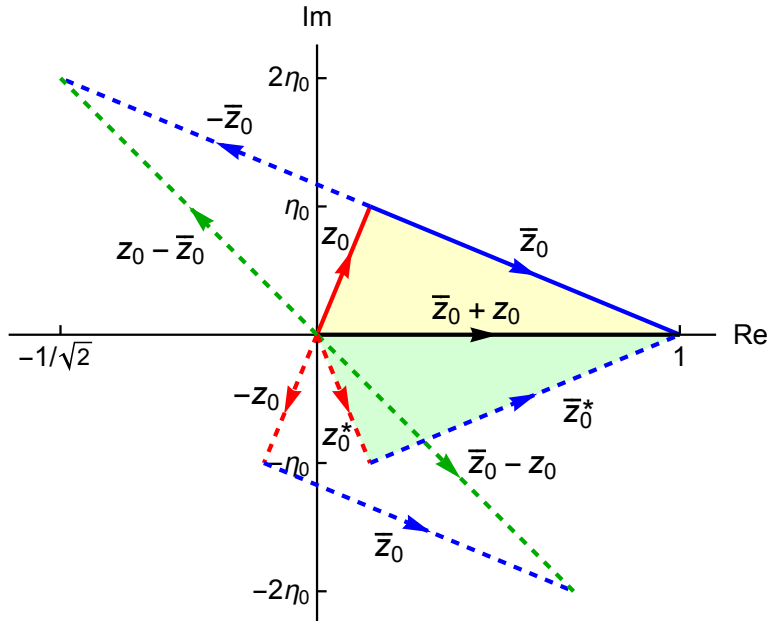


Figure 2. The leading-order UT, shaded yellow, and its CP transform (complex conjugate) in green. The two unshaded triangles, formed using $(-z_0, \bar{z}_0)$ and $(z_0, -\bar{z}_0)$ respectively, are both exactly congruent to the green one, each under a simple rotation, but only if the phase-difference between z_0 and \bar{z}_0 is $\frac{\pi}{2}$. Thus, in this case, they are equivalent to the CP transformation, since rotations of the UT are unobservable. This illustrates the invariance under the combined transformation of sign flip (of z_0 or \bar{z}_0) and CP .

complex-conjugate green. We recall that simultaneous phase changes of the off-diagonal elements of the MMs are unobservable and correspond to rotations of the unitarity triangle in the complex plane [28][29][30][31][32]. In the figure, we can see that a flip in the sign of z_0 alone results in a new LO-UT (unshaded) which is congruent to the CP -transformed triangle, being rotatable into it. The example with the triangle formed using z_0 and $-\bar{z}_0$ behaves similarly. Figure 2 thus makes manifest the symmetry under simultaneous CP transformation and single sign flip of either λ_q (but not both).

We emphasise that this symmetry is a direct result of the $\frac{\pi}{2}$ phase difference between z_0 and \bar{z}_0 . It is clear from figure 2 that if z_0 and \bar{z}_0 had any other phase difference, then forming a triangle using $-z_0$ and \bar{z}_0 or $(z_0$ and $-\bar{z}_0)$ would result in a triangle which was not congruent to the CP -transformed one, indicating that then, the symmetry is absent. One could reverse the argument and say that requiring such an invariance is sufficient to ensure that the two λ_q have a relative phase of $\frac{\pi}{2}$. The situation here is reminiscent of

that in many models of lepton mixing wherein invariance under a combined transformation involving CP and a second involution (e.g. $\mu - \tau$ exchange in [33]) results in a leptonic CP -phase close to $\frac{\pi}{2}$.

The above considerations extend to the case of the UT resulting from full diagonalisation, despite its being slightly perturbed relative to the LO one illustrated. This is verified using Jarlskog's CP -violating determinant [34][35], which, like the UT, *links* both MMs:

$$\mathcal{D} \equiv \text{Det}[M_u^0, M_d^0] = -2iF_uF_dJ_{CP}, \quad (6.1)$$

where $F_q \simeq (m_1^q - m_2^q)(m_2^q - m_3^q)(m_3^q - m_1^q)/(m_3^q)^3$. The determinant \mathcal{D} is readily shown to flip sign under either of the two λ_q sign reversals separately (given a λ_q phase difference of $\frac{\pi}{2}$), and of course under CP transformation. Interestingly, this latter check only works in the case of a texture in which the 13 and 31 elements of the MMs are zero (or have cubic powers in their respective λ_q), linking this invariance also to the texture zeroes. Thus, it seems that requiring invariance of the observables under the compound transformation also helps to constrain the form of the texture, beyond just the phase relationship of the λ_q .

We turn now to consider how the ratio λ_u/λ_d may be constrained to the value $\tan\frac{\pi}{8}$ by means of another invariance of the MMs. It is useful first to consider the more general situation where this is not the case (but the λ_q still retain their $\frac{\pi}{2}$ phase difference). Again the UT and Jarlskog's determinant are instrumental to the argument. Figure 3 illustrates the LO-UT for this relaxed texture, and we see that:

$$\left| \frac{\lambda_u}{\lambda_d} \right| = \left| \frac{z_0^*}{\bar{z}_0^*} \right| = \left| \frac{z_0}{\bar{z}_0} \right| = \tan \tilde{\beta}, \quad (6.2)$$

where $\tilde{\beta}$ is the CP -violating opening angle between \bar{z}_0 and $z_0 + \bar{z}_0$ in the complex plane (such that we still have the UT angle $\beta \simeq \tilde{\beta}$ after diagonalisation).

The Jarlskog determinant, eq. (6.1), is of course CP -violating and is a function of $\tilde{\beta}$. We find, for the generalised texture, the exact expression:

$$\mathcal{D} = -i\lambda_0^{10}b^2A_0^2\sin^3 2\tilde{\beta}f_{\mathcal{D}}(b, c_u, c_d, \lambda_0, \cos 2\tilde{\beta}) \quad (6.3)$$

($-\frac{\pi}{2} < \tilde{\beta} < \frac{\pi}{2}$), where $f_{\mathcal{D}}(b, c_u, c_d, \lambda_0, \cos 2\tilde{\beta})$ is a polynomial in $\cos(2\tilde{\beta})$. We consider now the following (observable) rotation of \bar{z}_0 in the complex plane:

$$2\tilde{\beta} \rightarrow 2\tilde{\beta} - \frac{\pi}{2}. \quad (6.4)$$

Under the transformation, eq. (6.4), we have that $\sin 2\tilde{\beta} \rightarrow -\cos 2\tilde{\beta}$ and $\cos 2\tilde{\beta} \rightarrow \sin 2\tilde{\beta}$, which obviously changes the value of \mathcal{D} , eq. (6.3), in general. However, in the particular case that $\tilde{\beta} = \beta_0 \equiv \frac{\pi}{8}$, the only effect is to flip the sign of $\sin 2\tilde{\beta}$ (and hence that of \mathcal{D}), effectively a CP transformation. This invariance can also be verified by inspecting figure 3. Symmetry can be restored again by performing a further explicit CP transformation (exactly analogous to the invariance under the compound λ_q sign flip and CP transformation discussed earlier). *Thus the symmetry of the texture which ensures $\tilde{\beta} = \beta_0 \equiv \frac{\pi}{8}$ is under the combined transformation, eq. (6.4) and CP .*

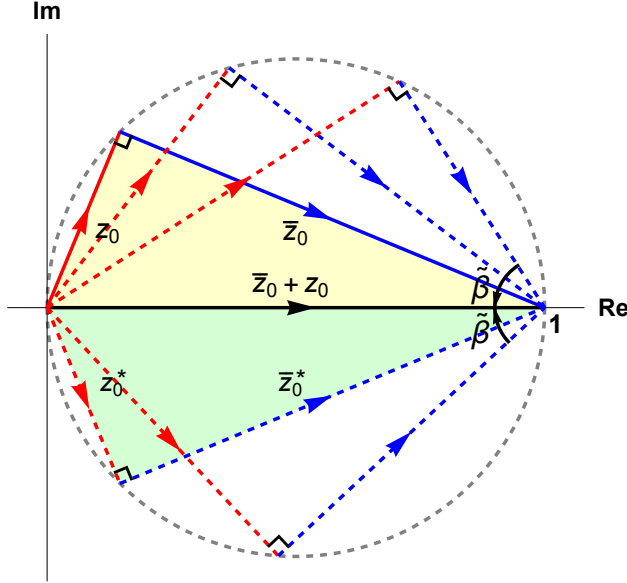


Figure 3. Leading-order UT, for our texture-pair (yellow, $\tilde{\beta} = \frac{\pi}{8}$), and (unshaded) three possible generalisations which represent a continuum with variable opening angle $\tilde{\beta}$ in the range $-\frac{\pi}{2} < \tilde{\beta} < \frac{\pi}{2}$ (negative values flip the sign of J_{CP}). The CP -conjugate LO-UT ($\tilde{\beta} = -\frac{\pi}{8}$) is shown in green. It is reachable by the particular $\tilde{\beta}$ rotation: $\tilde{\beta} \rightarrow \tilde{\beta} - \frac{\pi}{4}$, but only because $\tilde{\beta} = \beta_0 = \frac{\pi}{8}$. The figure is drawn in the PDG phase convention, although, since $\tilde{\beta}$ is a relative phase, the figure can be rotated between phase conventions. Note that $|\bar{z}_0 + z_0| = 1$ for all $\tilde{\beta}$ and for all phase conventions.

7 Discussion

In summary, we have introduced a novel texture for the two normalised quark mass matrices, having five free parameters in total. We use a small expansion parameter similar to Wolfenstein’s, but, motivated by the unitarity triangle, split in this case into two distinct complex components, λ_u and λ_d , whose complex sum is $\lambda + \mathcal{O}(\lambda^3)$. These complex components have ratio $\lambda_u/\lambda_d = -i \tan \frac{\pi}{8}$, which yields a UT consistent with experiment. In this “geometric” ansatz, the distinctiveness of the mass hierarchies for the two quark sectors, that of the “up” quarks being more extreme than that of the “down” quarks, is directly linked to the different magnitudes of the two sloped sides of the UT (i.e. $|V_{ub}| < |V_{td}|$) via the relation $|\lambda_u/\lambda_d| \simeq |V_{ub}|/|V_{td}| \simeq \tan \beta < 1$, which controls both. We obtain a good fit to the data renormalised to a scale in the range $(0.3 - 3) \times 10^4$ TeV at 68% CL.

We do not propose an extension of the SM with additional fields and quantum numbers to underpin the proposed texture, restricting our analysis to the phenomenology of the MMs themselves. Thus, we have instead elucidated two distinct new symmetries, manifested by the MMs, but absent from the SM, each involving an elementary transformation of the λ_q alone, with symmetry restored in each case by a CP transformation. We have shown that these symmetries are necessary and sufficient to constrain the UT angles to the experimentally-determined values. Whether these symmetries occur in isolation, or are a manifestation of some higher symmetry is, for the time being, unknown.

The up/down (weak isospin) reflection symmetry among the coefficients of the mass matrices is needed to reduce the number of parameters to make the ansatz more predictive, and is consistent with the data. The fact that two distinct parameters are needed in the smallest ‘11’ entry of the MMs is the least appealing aspect of the texture, but it is perhaps not entirely surprising, since radiative corrections due to the gauge interactions might dominate over the Yukawa contribution in this very small element and cannot be expected to be isospin-symmetric in the normalised mass matrices. Notwithstanding this feature, the proposed textures fit the experimental results and reduce the number of parameters needed to describe the data in the quark flavour sector from ten to seven (including the normalisations of the MMs).

A potentially useful and novel practical feature of the texture-pair is that among its input parameters and its fixed (by symmetry) constants, four of these seven quantities are directly and transparently seen to be equal in leading approximation to recognizable mixing observables, namely, $\lambda_0 \simeq \lambda$, $A_0 \simeq A$, $\rho_0 \simeq \rho$, $\eta_0 \simeq \eta$. The two identified compound symmetries are associated with the phenomenologically-successful UT relations $\alpha \simeq \frac{\pi}{2}$ and $\beta \simeq \frac{\pi}{8}$ respectively, and we have made precise numerical predictions for the angles of the UT (given in table 1), which can be tested by future experimental measurements.

Acknowledgements

It is a pleasure to thank Tim Gershon, Rama Krishnan, Chris Sachrajda and Jack Shergold for useful discussions and/or helpful comments on the manuscript. PFH acknowledges support from the UK Science and Technology Facilities Council (STFC) on the STFC consolidated grant ST/W000571/1.

A Analytic NLO solutions

For completeness, we provide here the algebraic NLO solutions of the texture:

$$\lambda = \lambda_0 \left[1 + \frac{f_\lambda}{4b} \lambda_0^2 \right] + \mathcal{O}(\lambda_0^5) \quad (\text{A.1})$$

$$A = A_0 \left[1 + \frac{1}{4b} (3b^2 - 2b\rho_0 - 2f_\lambda) \lambda_0^2 \right] + \mathcal{O}(\lambda_0^4) \quad (\text{A.2})$$

$$\bar{\rho} = \rho_0 \left\{ 1 - \frac{1}{8b\rho_0} [f_b + 2\eta_0(2f_a - 2b - 7b^2)] \lambda_0^2 \right\} + \mathcal{O}(\lambda_0^4) \quad (\text{A.3})$$

$$\bar{\eta} = \eta_0 \left\{ 1 - \frac{1}{4b} [2f_a - 4b + 3b^2 + 4\eta_0 f_b] \lambda_0^2 \right\} + \mathcal{O}(\lambda_0^4) \quad (\text{A.4})$$

where $f_\lambda = (3f_a - 5b + 4\eta_0 \delta_c)$, $f_a = A_0^2 + \frac{1}{2}(c_d + c_u)$, $f_b = b + \delta_c$ and $\delta_c = c_d - c_u$. The NLO corrections in eqs. (A.1)-(A.4) as fractions of the LO terms (calculated using the fitted values reported in table 1) are respectively: -5.8×10^{-3} , $+2.6\%$, $+3.6\%$ and -1.8% . For the mass ratios, we find:

$$\frac{m_1^q}{m_2^q} = -\lambda_q^2 (1 - r_q) \left\{ 1 + \left[r_A \frac{(2-r_q)}{(1-r_q)} - 2 \right] \lambda_q^2 \right\} + \mathcal{O}(\lambda_q^6) \quad (\text{A.5})$$

$$\frac{m_2^q}{m_3^q} = b \lambda_q^2 \left[1 + (1 - r_A) \lambda_q^2 \right] + \mathcal{O}(\lambda_q^6), \quad (\text{A.6})$$

where $r_q = \frac{c_q}{b}$ and $r_A = \frac{A_0^2}{b}$. The NLO corrections to the mass ratios m_c/m_t , m_s/m_b , m_u/m_c , m_d/m_s as a fraction of the LO terms are respectively -4.3×10^{-3} , -2.5% , $+4.3\%$, and $+4.5\%$ (calculated using the fitted values reported in table 1). In all cases, the results are compatible with the full numerical results reported in table 1, given the indicated degree of approximation.

References

- [1] H. Fritzsch, *Calculating the Cabibbo angle*, Phys. Lett. 70B, 436 (1977).
- [2] H. Fritzsch, *Weak-interaction mixing in the six-quark theory*, Phys. Lett. 73B (1978) 317.
- [3] H. Fritzsch, *Quark masses and flavor mixing*, Nucl. Phys. B155, 189 (1979).
- [4] P. Otto Ludl and W. Grimus, *A complete survey of texture zeros in general and symmetric quark mass matrices*, Phys. Lett. B 744 (2015) 38, e-Print: 1501.04942 [hep-ph].
- [5] W. Grimus et al, *Symmetry realization of texture zeros*, Eur. Phys. J. C, 36 (2004) 227, e-Print: arXiv:hep-ph/0405016.
- [6] C.D. Froggatt and H.B. Nielsen, *Hierarchy of quark masses, Cabibbo angles and CP violation*, Nucl. Phys. B 147 (1979) 277.
- [7] F. Feruglio, *Are neutrino masses modular forms?* in From My Vast Repertoire ...: Guido Altarelli's Legacy, A. Levy, S. Forte, Stefano, and G. Ridolfi, eds., pp.227–266, 2019, arXiv:1706.08749 [hep-ph].
- [8] H. Okada and M. Tanimoto, *Towards unification of quark and lepton flavors in A_4 modular invariance*, Eur. Phys. J. C 81 (2021) 1, 52, e-Print: 1905.13421 [hep-ph].
- [9] S. Kikuchi et al, *Texture zeros of quark mass matrices at fixed point $\tau = \omega$ in modular flavor symmetry*, Eur. Phys. J. C 83 (2023) 7, 591, e-Print: 2207.04609 [hep-ph].
- [10] S.J.D. King and S.F. King, *Fermion Mass Hierarchies from Modular Symmetry*, JHEP 09 (2020) 043, e-Print: 2002.00969 [hep-ph].
- [11] C. Jarlskog, R. Stora, *Unitarity polygons and CP violation areas and phases in the standard electroweak model*, Phys. Lett. B, 208 (1988), 268.
- [12] James D. Bjorken, *On the determination of phases of generalized Kobayashi-Maskawa matrix elements from their magnitudes*, Phys. Rev. D 39 (1989) 1396.
- [13] I. Masina and C.A. Savoy, *Real and imaginary elements of fermion mass matrices*, Nucl. Phys. B 755 (2006) 1, e-Print: arXiv: hep-ph/0603101.
- [14] P.F. Harrison, D.R.J. Roythorne and W.G. Scott, *Is the Unitarity Triangle Right?*, Contribution to PANIC 08, (2008) 756, e-Print: 0904.3014 [hep-ph].
- [15] S. Antusch et al, *Quark mixing sum rules and the right unitarity triangle*, Phys. Rev. D 81 (2010) 033008, e-Print: 0910.5127 [hep-ph].
- [16] S. Navas et al. (Particle Data Group), *The Review of Particle Physics*, Phys. Rev. D 110, 030001 (2024).
- [17] We are grateful to Tim Gershon, who first pointed-out to us to the closeness of β to $\frac{\pi}{8}$, private communication.

- [18] L. Wolfenstein, *Parametrization of the Kobayashi-Maskawa matrix*, Phys. Rev. Lett. 51 (1983) 1945.
- [19] A.J. Buras, M.E. Lautenbacher and G. Ostermaier, *Waiting for the Top quark mass, $K^+ \rightarrow \pi^+ \nu \bar{\nu}$, $B_s^0 - \bar{B}_s^0$ mixing and CP asymmetries in B-decays*, Phys. Rev. D50 (1994) 3433, [hep-ph/9403384].
- [20] Y. Aoki et al. (Flavour Lattice Averaging Group (FLAG)), *FLAG Review 2024*, CERN-TH-2024-192, e-Print: arXiv:2411.04268.
- [21] B. Belfatto and Z. Berezhiani, *Minimally modified Fritzsch texture for quark masses and CKM mixing*, JHEP 08 (2023) 162, e-Print: arXiv:hep-ph/2305.00069.
- [22] M.E. Machacek, M.T. Vaughn, *Two Loop Renormalization Group Equations in a General Quantum Field Theory: 1. Wave Function Renormalization*, Nucl. Phys. B 222 (1983) 83.
- [23] M.E. Machacek, M.T. Vaughn, *Two Loop Renormalization Group Equations in a General Quantum Field Theory: (II). Yukawa Couplings*, Nucl. Phys. B 236 (1984) 221.
- [24] M.E. Machacek, M.T. Vaughn, *Two Loop Renormalization Group Equations in a General Quantum Field Theory: (III). Scalar Quartic Couplings*, Nucl. Phys. B, 249 (1985) 70.
- [25] C. Balzereit et al, *The Renormalization Group Evolution of the CKM Matrix*, Eur. Phys. J. C 9 (1999) 197, e-Print: hep-ph/9810350 [hep-ph].
- [26] P. Kielanowski, S. Rebeca Juarez Wysozka, *Renormalization group evolution of the CKM matrix*, AIP Conf.Proc. 670 (2003) 1, 81, e-Print: hep-ph/0301098.
- [27] R. Krishnan, "The framework of the auxiliary group: two birds with one stone" (2023), arXiv:2309.11542 (hep-ph).
- [28] C. Jarlskog, *Matrix representation of symmetries in flavor space, invariant functions of mass matrices, and applications*, Phys. Rev. D 35 (1987) 1685;
- [29] C. Jarlskog, *Flavor projection operators and applications to CP violation with any number of families*, Phys. Rev. D36 (1987) 2128.
- [30] C. Jarlskog and A. Kleppe, *Measurables of the quark mixing matrix as invariant functions of mass matrices*, Nucl. Phys. B286 (1987) 245.
- [31] C.H. Albright, C. Jarlskog and B-A. Lindholm, *Testing the Fritzsche quark mass matrices with the invariant function approach*, Phys. Lett. B199 (1987) 553;
- [32] C.H. Albright, C. Jarlskog and B-A. Lindholm, *Three-family Fritzsche and Stech models with minimal and two-doublet Higgs structures*, Phys. Rev. D38 (1988) 872.
- [33] P.F. Harrison, W.G. Scott, *μ - τ reflection symmetry in lepton mixing and neutrino oscillations*, Phys. Lett. B 547 (2002) 219, e-Print: hep-ph/0210197 [hep-ph]
- [34] C. Jarlskog, *Commutator of the Quark Mass Matrices in the Standard Electroweak Model and a Measure of Maximal CP Nonconservation*, Phys. Rev. Lett. 55 (1985) 1039.
- [35] C. Jarlskog, *A Basis Independent Formulation of the Connection Between Quark Mass Matrices, CP Violation and Experiment*, Z. Phys. C29 (1985) 491.